ORIGINAL RESEARCH • GASTROINTESTINAL IMAGING

Radiology

Noninvasive Staging of Liver Fibrosis Using 5-Minute Delayed Dual-Energy CT: Comparison with US Elastography and Correlation with Histologic Findings

Uday Kumar Marri, MD • Prasenjit Das, MD • Shalimar, DM • Mani Kalaivani, PhD • Deep Narayan Srivastava, MD • Kumble Seetharama Madhusudhan, MD, FRCR

From the Departments of Radiodiagnosis and Interventional Radiology (U.K.M., D.N.S., K.S.M.), Pathology (P.D.), Gastroenterology (Shalimar), and Biostatistics (M.K.), All India Institute of Medical Sciences, Ansari Nagar, New Delhi 110029, India. Received May 19, 2020; revision requested July 6; revision received October 21; accepted November 2. **Address correspondence to** K.S.M. (e-mail: *drmadhuks@gmail.com*)

Conflicts of interest are listed at the end of this article.

See also the editorial by Chandarana and Shanbhogue in this issue.

Radiology 2021; 298:600–608 • https://doi.org/10.1148/radiol.2021202232 • Content codes: GI CT

Background: Normalized iodine concentration (NIC) (ratio of iodine concentration of liver to that of aorta) of liver at delayed dual-energy CT (DECT) may reflect the amount of fibrosis based on the extent of iodine uptake.

Purpose: To stage liver fibrosis by using 5-minute delayed DECT and compare findings with those of transient elastography (TE), shear-wave elastography (SWE), and histologic examination.

Materials and Methods: This prospective study included patients with chronic liver disease who were scheduled to undergo multiphase abdominal CT and liver biopsy from January 2017 to September 2018. Fifty individuals being screened as renal donors comprised the control group. Study participants underwent TE, SWE, multiphasic DECT (including 5-minute delayed dual-energy scanning), and liver biopsy. Multiphasic DECT and SWE were performed in the control group. The NIC of the right lobe of the liver (RNIC) was compared with liver stiffness (LS) as measured with TE and SWE and with the METAVIR fibrosis stage (ranging from F0 to F4). Diagnostic performance was assessed by using areas under the receiver operating characteristic curve (AUCs).

Results: A total of 107 participants (mean age, 35 years ± 12 [standard deviation]; 57 men) and 50 control subjects (mean age, 47 years ± 11; 29 women) were evaluated. The RNIC showed strong correlation with METAVIR stage (Spearman ρ = 0.81, $P <$ .001). The AUC for RNIC with each METAVIR stage ranged between 0.86 (95% CI: 0.76, 0.97) and 0.96 (95% CI: 0.92, 0.99). The cut-off value of RNIC was 0.24 (sensitivity: 85% [86 of 101 participants; 95% CI: 77%, 91%]; specificity: 83% [84 of 101 participants; 95% CI: 42%, 98%]) for stage F1 fibrosis and 0.29 (sensitivity: 84% [67 of 80 participants; 95% CI: 74%, 90%]; specificity: 81% [65 of 80 participants; 95% CI: 63%, 92%]) for stage F2 fibrosis. RNIC correlated well with LS as measured with TE and SWE (Spearman ρ = 0.60 and 0.64, respectively; $P <$ .001).

Conclusion: Normalized iodine concentration of liver at 5-minute delayed dual-energy CT showed strong correlation with the histologic stages of liver fibrosis and good diagnostic performance in estimating liver fibrosis.

Online supplemental material is available for this article.

Chronic liver disease is a growing public health problem worldwide and is associated with clinically significant morbidity and mortality (1). About 12%–44% of cases of chronic liver disease eventually progress to advanced fibrosis and cirrhosis at variable rates, leading to complications and worsening of prognosis (2,3). An early diagnosis of liver fibrosis would assist in taking the necessary steps in management to halt, and sometimes even reverse, the progression of fibrosis (4). Hence, the assessment of the severity of liver fibrosis has direct implications in the treatment, follow-up, and risk stratification of these patients (1,5).

Liver biopsy is the current reference standard for quantifying liver fibrosis (6). Although it provides information beyond fibrosis, biopsy has many downsides. In addition to being invasive, biopsy has the risk of hemorrhagic complications and is subject to sampling errors. Also, sampling is difficult owing to small and hard liver in advanced disease, and interobserver variations exist (7,8). Repeat biopsy to assess alterations in fibrosis is unjustified. Therefore, there exists a substantial need for the development of a simple, noninvasive, repeatable, and reproducible test for the assessment of liver fibrosis.

Tests for the serum markers used to assess the severity of liver fibrosis are expensive and tedious, with sensitivity and specificity ranging from 33% to 96% and 29% to 100%, respectively (9,10). In contrast, transient elastography (TE) and shear-wave elastography (SWE), which enable assessment of liver fibrosis by measuring liver stiffness (LS), are simple and accurate. However, they are affected by ascites, obesity, biliary obstruction, acute inflammation, fatty liver, and narrow intercostal spaces (11,12). Similar to liver biopsy, only a small volume of the liver is sampled. Although accurate, MR elastography is expensive and cumbersome, is not widely available, and requires additional hardware (13–15).

Dual-energy CT (DECT) is an advancement in the field of CT wherein images are acquired at two different energies (kilovolts) and a "multimaterial decomposition"

Abbreviations

AUC = area under the receiver operating characteristic curve, CPA = collagen proportionate area, DECT = dual-energy CT, LNIC = NIC of the left lobe of the liver, LS = liver stiffness, NIC = normalized iodine concentration, RNIC = NIC of the right lobe of the liver, ROI = region of interest, SWE = shear-wave elastography, TE = transient elastography

Summary

Five-minute delayed dual-energy CT had a high positive correlation with histologic fibrosis scores and showed good diagnostic performance in estimating liver fibrosis.

Key Results

- Normalized iodine concentration of the right lobe of the liver (RNIC) at 5-minute delayed dual-energy CT showed a strong positive correlation with histologic fibrosis scores (Spearman ρ = 0.81, $P < .001$).
- In the differentiation of different METAVIR stages, RNIC showed areas under the receiver operating characteristic curve ranging from 0.86 to 0.96.
- RNIC had good agreement with liver stiffness as measured with transient elastography and shear-wave elastography (Spearman ρ = 0.60 and 0.64, respectively; $P < .001$).

algorithm is used to differentiate and quantify various materials such as fat, soft tissue, and iodine in a given pixel (16,17). DECT enables assessment of the severity of liver fibrosis by means of contrast-enhanced delayed acquisition (18,19). We hypothesized that the fibrous tissue in the diseased liver would tend to retain iodinated contrast material for a longer period than would the normal liver tissue. Hence, the iodine concentration of liver on a delayed DECT scan should quantify fibrosis (18,19). Only a few small studies on the role of DECT in the assessment of liver fibrosis in chronic liver disease are available in the literature. This study aimed to evaluate the usefulness of DECT in the staging of liver fibrosis in chronic liver disease by comparing it with TE, SWE, and histologic examination.

Materials and Methods

Participants

This prospective study was approved by the institutional ethics committee, and written informed consent for the study was obtained from all participants, including the control subjects. The study included consecutive patients who were known to have or suspected of having chronic liver disease and who were scheduled to undergo multiphase abdominal CT and liver biopsy from January 2017 to September 2018. The exclusion criteria were portal vein thrombosis, Budd-Chiari syndrome, no biopsy or inadequate biopsy, recent history of decompensated hepatic failure, and contraindications to iodinated contrast material (renal derangement, allergy). All included patients underwent DECT, TE, SWE, and liver biopsy. The control participants were voluntary renal donors.

DECT Liver Acquisition

DECT was performed with a second-generation dual-source DECT scanner (Definition Flash; Siemens Healthineers) with tube voltages of 100 kVp and 140 kVp and with a tin filter and automated dose reduction technique (CARE Dose4D; Siemens Healthineers). The CT parameters used were as follows: detector collimation, 64 × 0.6 mm; gantry rotation time, 0.5 second; pitch, 0.6; matrix, 512 × 512; reconstruction thickness, 1.5 mm; reconstruction interval, 1.5 mm; reconstruction plane, axial; and reconstruction kernel, D30f. A dose of 1.5 mL per kilogram body weight of nonionic iodinated contrast material (Iomeron [Bracco], 400 mg/mL; or Omnipaque [GE Healthcare], 350 mg/mL) was administered intravenously at 4 mL/sec with an automated injector system followed by acquisition of images in three phases. After the standard late arterial and portal venous phases, images in the delayed phase were acquired at 225 seconds after the portal venous phase (total delay = 5 minutes) in dual-energy mode, covering the liver.

DECT Image Analysis

The 5-minute delayed images were then transferred to a dedicated workstation (syngo.via, version VB10B, 2016; Siemens Healthineers) for dual-energy analysis by two radiologists (U.K.M. and K.S.M., with 3 and 12 years of experience in abdominal radiology, respectively) in consensus. In case of disagreement between the two readers, a third radiologist (D.N.S., with 30 years of experience in abdominal radiology) analyzed the case, and his findings were considered final. All three radiologists were blinded to the clinical and histologic information. Three dual-energy regions of interest (ROIs), each measuring 2 cm in diameter, were drawn on different areas of the right and left lobes of the liver separately, avoiding major vessels and any focal lesions (Fig 1). On the right lobe, the ROIs were drawn in the area that approximately matched the area of biopsy. On the left lobe, one ROI each was placed at the levels of the left hepatic vein origin and the left portal vein and below the level of the left portal vein. The software generated the iodine concentrations within each ROI, representing both intravascular and extravascular iodine. Another ROI was placed on the abdominal aorta at the level of the celiac trunk. Then the normalized iodine concentration (NIC), the ratio of mean iodine concentration of liver to iodine concentration of aorta, was calculated (to exclude intravascular iodine component) for the right (NIC of the right lobe of the liver [RNIC]) and the left (NIC of the left lobe of the liver [LNIC]) lobes of the liver. The means of three values of RNIC and LNIC were used for evaluation. After virtual monochromatic images were generated between the energies 40 keV and 190 keV, the CT attenuation values (Hounsfield units) in the same ROIs of the right lobe of the liver were measured at 40 keV and 70 keV, and the slope of the monochromatic spectral curve was calculated by using the formula $(CT_{40keV} - CT_{70keV})/30$, as suggested by Wei et al (20) in their study of renal masses (Fig 1, *C*). The mean of the three values was used for analysis.

TE Procedure

TE was performed with FibroScan (Echosens) with an M+ or XL+ probe by an operator with more than 2 years of experience. The LS (in kilopascals) was recorded through the right lower intercostal spaces from the right lobe of the liver by using the standard technique. The procedure was performed with the

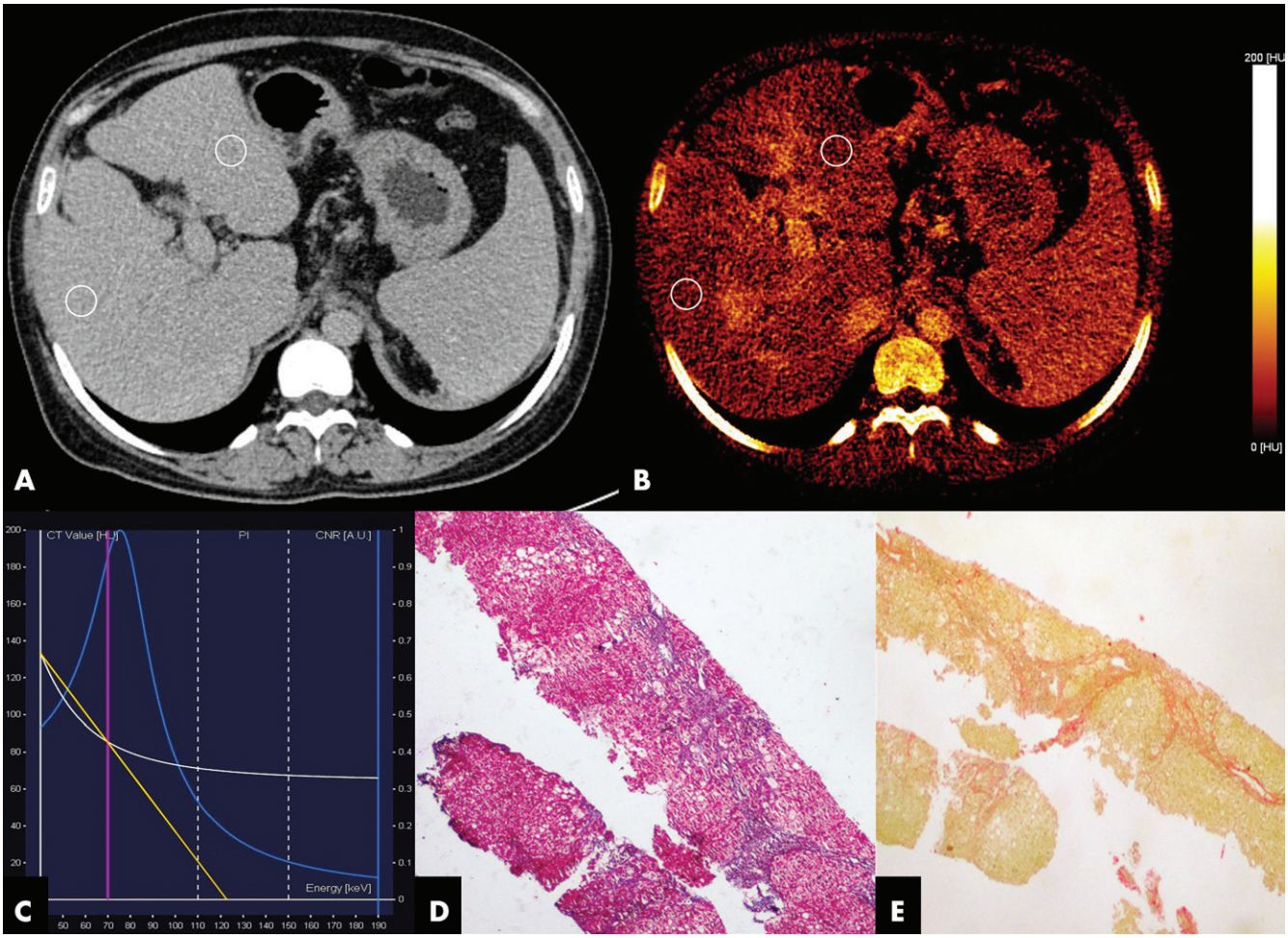

Figure 1: Images in a 26-year-old woman with autoimmune hepatitis. *A*, Axial delayed phase dual-energy CT (DECT) image through liver with regions of interest (ROIs) in both lobes. Iodine concentrations were 0.9, 0.8, and 0.9 mg/mL in the right lobe and 0.9, 0.7, and 1 mg/mL in the left lobe. In the abdominal aorta, the iodine concentration was 2.4 mg/mL. The normalized iodine concentrations of the right and left lobes of the liver were 0.38 and 0.29, respectively. *B*, Iodine map from delayed phase shows heterogeneous iodine uptake in liver. *C*, Graph shows monochromatic spectral curve at DECT. White line represents curve of ROI. Blue line is iodine reference curve. Yellow line is slope of monochromatic spectral curve measured in study, which was 1.29 HU/keV. *D*, Photomicrograph of biopsy sample (Masson trichrome stain; original magnification, ×40) shows METAVIR stage F3 fibrosis. *E*, Photomicrograph (Sirius red stain; original magnification, ×40) shows collagen proportionate area of 6.7%. Liver stiffness was 13.5 kPa with transient elastography and 13.4 kPa with shear-wave elastography.

participants in a supine position with the right arm abducted, and the probe was placed in the right lower intercostal space after percussion to confirm the position of the liver. Ten valid measurements were obtained at the same location, and the median was noted. The LS measurement was considered unreliable if the success rate was less than 60% or the ratio of the interquartile range of LS to the median was more than 30%.

Two-dimensional SWE Procedure

SWE was performed with the Aixplorer US system (SuperSonic Imagine) with an SC1-6 convex probe by a radiologist with 3 years of experience (U.K.M.), on the same day as DECT. The operator was blinded to the participant's clinical information. SWE was performed with the standard technique (12). With the participant in the supine position with the right arm abducted, the probe was placed over the right lateral intercostal spaces to enable visualization of the liver. Then, an SWE box was placed over the liver (2–5 cm deep to liver capsule) and the image was frozen when it showed homogeneous color filling, with the participant's breath held in expiration. A circular ROI (called Q-box, 1 cm in diameter) was placed within the SWE box to obtain the LS (in kilopascals). The stabilization index, which indicates reliability of the measurement, was maintained above 90% as recommended by the manufacturer. Three such values were obtained from the same region of the liver, and the median was noted.

Biopsy

Liver biopsy was performed with an 18-gauge needle in the right lobe of the liver by using either the percutaneous or transjugular route, depending on the patient's clinical condition. This was used as the reference standard. The sample was evaluated by a pathologist (P.D., with 12 years of experience in gastrointestinal pathology) who was blinded to clinical and radiologic information. The biopsy sample was considered inadequate if the core size was less than 1.5 cm or if it showed fewer than 10 complete portal tracts. The stage of fibrosis was defined by using the standard METAVIR classification, from F0 (no

fibrosis) to F4 (cirrhosis). The histologic stages of fibrosis were also grouped into normal (F0), mild fibrosis (≥F1), significant fibrosis (≥F2), advanced fibrosis (≥F3), and cirrhosis (F4) groups (Fig 1, *D*). Objective quantification of fibrosis in the sample was also done after the sample was stained with Sirius red stain and by using image analysis software (Image Pro-Plus, version 6.1; Media Cybernetics). The software automatically calculated the collagen proportionate area (CPA) as a percentage of the sample (Fig 1, *E*).

Control Group

Fifty volunteer kidney donors who had normal liver function test results and LS of less than 7 kPa were included as control participants and underwent multiphase DECT of the abdomen with the same protocol. The RNIC, LNIC, and slope of monochromatic spectral curve were measured in the same manner as in the participants with chronic liver disease, and the mean values were calculated. SWE of the liver was performed on the same day, and the median LS value was noted.

Statistical Analysis

Statistical analysis was performed with software (Stata Statistical Software: Release 14; StataCorp). Descriptive statistics were used to describe the demographic characteristics of participants with chronic liver disease and the control group. The RNIC, LNIC, slope of monochromatic spectral curve, and LS values obtained with SWE and TE were compared with the stage of fibrosis and the CPA at histologic examination by using Spearman correlation analysis for nonnormal distribution data. DECT parameters and LS at SWE of the control group were compared with those of participants with chronic liver disease by using Wilcoxon rank-sum and Mann-Whitney tests. Areas under the receiver operating characteristic curve (AUCs) were generated for each, and the cut-off values of various parameters were defined. $P < .05$ was considered to indicate a statistically significant difference.

Results

Participant Characteristics

Among 133 participants with chronic liver disease who underwent DECT, 22 were excluded (portal vein thrombosis [$n = 4$], Budd-Chiari syndrome [$n = 2$], absence of biopsy [$n = 16$]). Subsequently, 111 participants underwent DECT, SWE, and liver biopsy. The liver biopsy samples of four participants were inadequate for histologic assessment; hence, these patients were excluded. Finally, 107 participants with chronic liver disease (mean age, 35 years ± 12 [standard deviation]; 57 men) were included in the study for analysis (Fig 2). Fifty volunteer kidney donors (mean age, 47 years ± 11; 29 women) were used as the control group. The demographic characteristics of participant and control groups are shown in Table 1. DECT analysis and SWE were successful in all 107 participants with liver disease. However, TE failed in six participants. The results of the study are summarized in Table 2. The average time between TE and DECT and/or SWE, DECT and/or SWE and biopsy, and TE and biopsy were 25 days ± 20, 37 days ± 12, and 61 days ± 17, respectively.

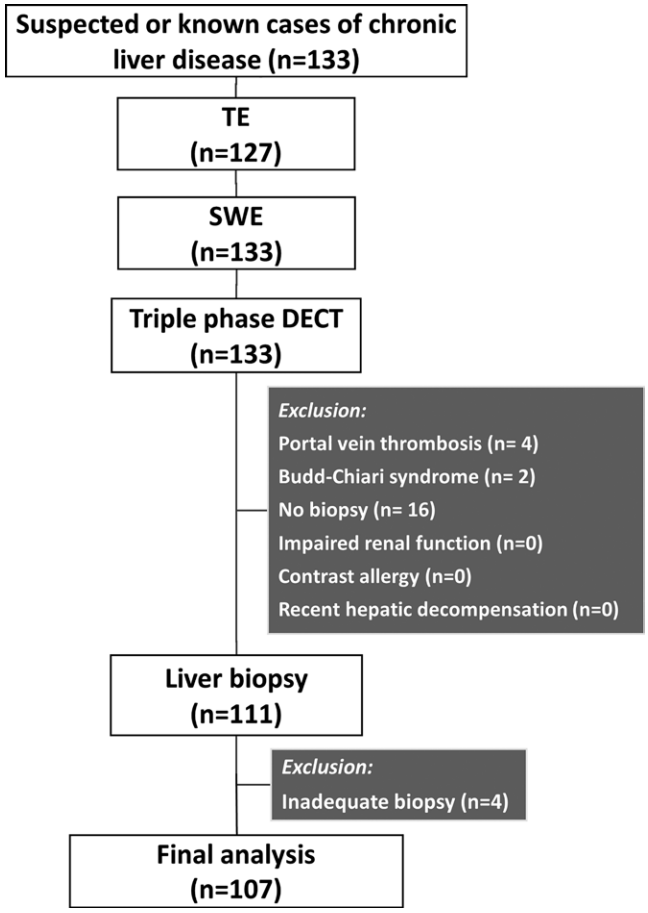

Figure 2: Study flowchart. DECT = dual-energy CT, SWE = shear-wave elastography, TE = transient elastography.

DECT in the Staging of Liver Fibrosis

The mean RNIC correlated well with the METAVIR stages and CPA (Spearman ρ = 0.81 and 0.67, respectively; $P < .001$) (Fig 3). Similarly, the mean LNIC showed good positive correlation with the stage of fibrosis (Spearman ρ = 0.72, $P < .001$) and with CPA (Spearman ρ = 0.66, $P < .001$). However, the slope of monochromatic spectral curve correlated weakly with the histologic stage of fibrosis (Spearman ρ = 0.27, $P = .006$) and did not correlate with the CPA (Spearman ρ = 0.30, $P = .12$). The absolute iodine concentration of the right lobe was also compared with histologic findings, and it showed a Spearman correlation coefficient of 0.67 ($P < .001$).

The receiver operating characteristic curves for the RNIC, LNIC, and slope of monochromatic spectral curve were generated for different fibrosis groups (Fig 4, Fig E1 [online]). The RNIC showed the highest AUC among the DECT parameters, ranging from 0.86 in differentiating F0 and F1–4 stages to 0.96 in differentiating F4 and F0–3 fibrosis stages. RNIC rather than LNIC was used for a more accurate comparison, as the biopsy samples had been obtained from the right lobe. Furthermore, in the differentiation of F0 from F1–F3, the AUC was 0.84 (95% CI: 0.72, 0.96) for RNIC and 0.81 (95% CI: 0.64, 0.98) for

Table 1: Demographic and Clinical Characteristics of Participants with Chronic Liver Disease and Control Subjects

Parameter	Participants	Control Group
No. of participants	107	50
No. of men	57	21
No. of women	50	29
Age (y)*		
Overall	35 ± 12	47 ± 11
Men	33 ± 11	49 ± 13
Women	38 ± 12	44 ± 9
Cause of chronic liver disease		
Autoimmune hepatitis	27	
Nonalcoholic fatty liver disease	22	
Chronic hepatitis B	18	
Chronic hepatitis C	6	
Noncirrhotic portal hypertension	9	
Alcoholic liver disease	6	
Primary biliary cirrhosis	3	
Drug-induced liver disease	2	
Hemochromatosis	1	
Wilson disease	1	
Cryptogenic cirrhosis	12	

Note.—Except where indicated, data are numbers of participants.
* Data are means ± standard deviations.

LNIC; in the differentiation of F0–F1 from F2–F3, the AUC was 0.88 (95% CI: 0.80, 0.96) for RNIC and 0.86 (95% CI: 0.76, 0.95) for LNIC. In the latter, the optimal cut-off value was 0.26 (sensitivity, 89%; specificity, 73%) for RNIC and 0.29 (sensitivity, 79%; specificity, 73%) for LNIC.

In participants with fatty liver (n = 22), the RNIC and LNIC showed lower correlation with METAVIR stage (Spearman ρ = 0.71 and 0.70, respectively; $P < .001$). In the remaining patients (n = 85), the correlation of RNIC and LNIC with METAVIR stage was slightly better (Spearman ρ = 0.83 and 0.73, respectively; $P < .001$). However, this difference was not statistically significant ($P = .50$). We did not evaluate the impact of liver fat on the diagnostic performance of NIC, TE, and SWE because there were few participants with fatty liver at each METAVIR stage (stage F0, n = 2; stage F1, n = 4; stage F2, n = 12; stage F3, n = 2; stage F4, n = 2) and histologic quantification of fat was not performed.

The intraclass correlation coefficients for the reliability of NIC measurements among three ROIs in the right and left lobes were 0.78 (95% CI: 0.71, 0.84) and 0.76 (95% CI: 0.69, 0.82), respectively.

The RNIC showed a positive correlation with LS values measured with TE as well as with SWE (Spearman ρ = 0.60 and 0.64, respectively; $P < .001$).

Comparison between RNIC and LNIC

Overall, the LNIC showed good positive correlation with the RNIC (Spearman ρ = 0.81, $P < .001$). However, when correlation was made between them for each fibrosis stage, the correlation coefficients in stages F0, F1, F2, F3, and F4 were 0.98, 0.66, 0.57, 0.55, and 0.71, respectively, indicating heterogeneous fibrosis distribution in the intermediate stages. In the control group, there was excellent correlation between the RNIC and the LNIC (r = 0.91, $P = .005$). Although AUCs for different METAVIR stages were slightly higher for RNIC compared with LNIC, they did not indicate a statistically significant difference except in differentiating F4 from other fibrosis groups (comparison P values for groups ≥F1, ≥F2, ≥F3, and F4 were .61, .58, .08, and .01, respectively).

LS in Liver Fibrosis Staging

The LS values measured with TE and SWE showed good positive correlation with the histologic stages of fibrosis (Spearman ρ = 0.70 and 0.74, respectively; $P < .001$) and with CPA (Spearman ρ = 0.64 and 0.59, respectively; $P < .001$) (Fig 3). The AUC of LS measured with TE and SWE for each histologic group ranged from 0.79 to 0.98 (Fig 4, Fig E1 [online]).

The LS values measured with TE and SWE showed high agreement with each other (Spearman ρ = 0.66, $P < .001$) (Fig 3). There were no technical failures with SWE, whereas TE had a failure rate of 5.6% (six of 107 participants). SWE showed slightly better correlation with histologic assessment than TE (Spearman ρ for SWE = 0.74 vs TE = 0.70), but the difference was not statistically significant ($P = .27$).

Although the AUCs were slightly higher for RNIC compared with TE and SWE, they mostly did not indicate a statistically significant difference. In the differentiation of greater than or equal to F1, greater than or equal to F2, greater than or equal to F3, and F4 groups from the rest, the comparison P values of RNIC and TE were .82, .79, .05, and .10, and of RNIC and SWE were .02, .82, .16, and .02, respectively. The cut-off values of RNIC and LS values as measured with TE and SWE for significant fibrosis, advanced fibrosis, and cirrhosis are shown in Table 3. The values of RNIC and LS as measured with TE and SWE in the differentiation of early stages of fibrosis are shown in Table 4.

The mean RNIC in the control group (0.23 ± 0.07) differed from the corresponding values in participants with F2 (0.31 ± 0.06), F3 (0.39 ± 0.06), and F4 (0.56 ± 0.20) fibrosis ($P < .001$). However, the mean RNIC between the control group (0.23 ± 0.07) and the participants with stage F1 fibrosis (0.23 ± 0.07) was not different ($P = .95$). Figure 3 shows the distribution of the values of RNIC and LS as measured with SWE and TE in different fibrosis stages and in the control group. The RNIC of control subjects had a wider range and significant overlap with F0–F2 stages compared with LS as assessed with SWE.

Discussion

The current prospective single-center study evaluated the accuracy of normalized iodine concentration (NIC) of liver measured with 5-minute delayed dual-energy CT (DECT) for staging liver fibrosis, with histologic examination as a reference standard. The study showed that, in staging liver fibrosis, the accuracy of NIC at DECT was similar to that of liver stiffness measurements derived with transient elastography and shear-wave elastography. The NIC of the right lobe of the liver (RNIC) showed good correlation with the histologic fibrosis

Table 2: Distribution of Quantitative Imaging Parameters in the Control Group and Participants with Chronic Liver Disease at Different Stages of Fibrosis

Fibrosis Stage	CPA (%)*	RNIC*	LNIC*	Liver Stiffness (kPa)†		Slope of Monochromatic Spectral Curve (HU/keV)*
				TE	SWE	
Control group (n = 50)	…	0.23 ± 0.07 (0.03–0.39)	0.27 ± 0.08 (0.05–0.44)	…	5.30 (4.10–6.50)	1.73 ± 0.56 (1.18–3.68)
F0 (n = 6)	0.89 ± 1.49 (0.04–3.90)	0.22 ± 0.05 (0.14–0.30)	0.23 ± 0.10 (0.06–0.33)	5.95 (4.50–9.0)	5.40 (4.30–5.60)	1.60 ± 0.23 (1.25–1.90)
F1 (n = 21)	0.67 ± 0.53 (0.002–2.30)	0.23 ± 0.07 (0.06–0.38)	0.26 ± 0.07 (0.13–0.46)	6.85 (5.20–8.60)	7.30 (6.40–8.70)	1.71 ± 0.71 (0.46–3.47)
F2 (n = 34)	2.37 ± 2.08 (0.20–8.30)	0.31 ± 0.06 (0.20–0.48)	0.33 ± 0.06 (0.24–0.50)	11.75 (8.90–14.30)	9.20 (7.40–12.70)	1.56 ± 0.69 (0.27–3.42)
F3 (n = 31)	6.04 ± 4.05 (0.40–16.80)	0.39 ± 0.06 (0.21–0.49)	0.41 ± 0.07 (0.27–0.57)	13.35 (11.80–17.10)	13.30 (11.60–18.90)	1.68 ± 0.67 (1.18–2.84)
F4 (n = 15)	14.2 ± 6.05 (1.20–22.50)	0.56 ± 0.20 (0.40–1.10)	0.56 ± 0.20 (0.38–1.15)	21.00 (16.6–44.9)	22.20 (11.10–34.70)	2.31 ± 0.81 (0.83–3.68)

Note.—CPA = collagen proportionate area, LNIC = normalized iodine concentration of the left lobe of the liver, RNIC = normalized iodine concentration of the right lobe of the liver, SWE = shear-wave elastography, TE = transient elastography.

* Data are means ± standard deviations, with range in parentheses.

† Data are medians, with the interquartile range in parentheses.

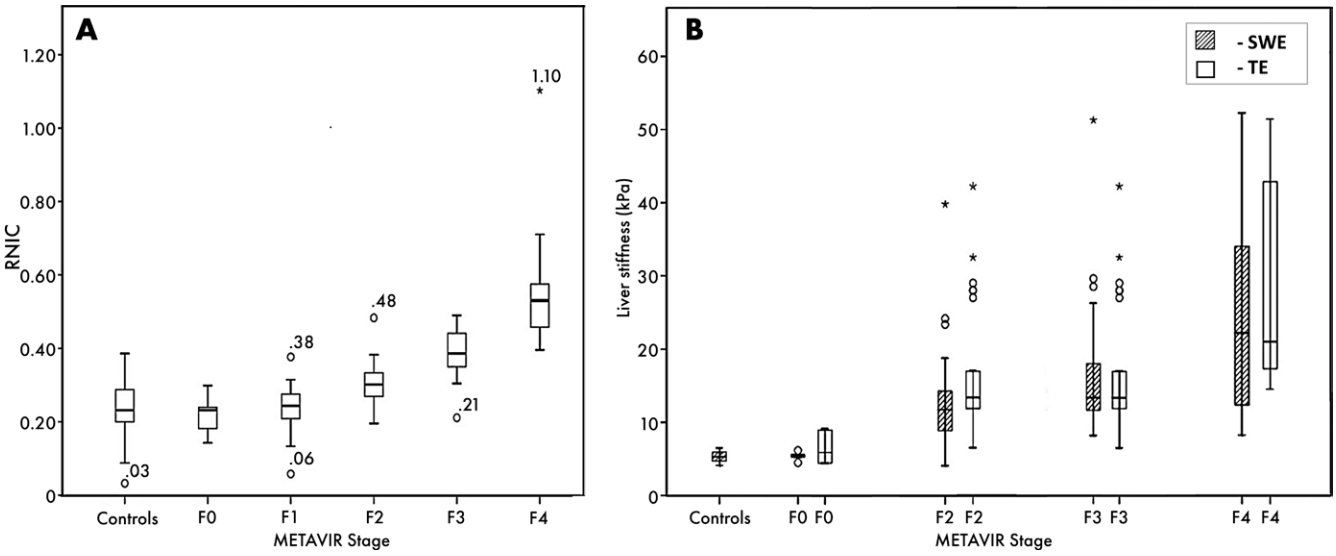

Figure 3: *A*, Box plot shows distribution of normalized iodine concentration of the right lobe of the liver (RNIC) in control subjects and participants with different METAVIR stages. Number are RNIC values of outliers (O) and extreme outlier (*). *B*, Box plot shows distribution and comparison of liver stiffness values as measured with shear-wave elastography (SWE) and transient elastography (TE) in control subjects and participants with different METAVIR stages. O = outliers, * = extreme outliers.

stage (Spearman ρ = 0.81, $P < .001$). Sensitivity and specificity of the RNIC in predicting the various stages of fibrosis were in the range of 83%–93% and 81%–87%, respectively. There was good intra-observer reliability for RNIC and NIC of the left lobe of the liver, with intraclass correlation coefficients of 0.78 and 0.76, respectively.

Late contrast enhancement of the liver parenchyma in patients with chronic hepatitis was first demonstrated by Semelka et al (21) in 2001. In their retrospective study, they compared 5–10-minute delayed gadolinium-enhanced images of the liver and histologic fibrosis in 29 patients with chronic hepatitis and found that the delayed gadolinium enhancement correlated linearly and highly with liver fibrosis (sensitivity, 73%; specificity, 66%). Evaluation of late contrast enhancement by using iodinated contrast material and CT relies on a similar principle. Lamb et al (18) found that NIC on 3-minute delayed DECT images correlated with Ishak fibrosis stage in 12 individuals ($P < .05$). Fuentes et al (22) also showed a strong correlation between NIC in the delayed phase and histologic findings in 18 individuals (Spearman ρ = 0.77, $P = .001$). Lv et al (19) showed that NIC at portal venous phase DECT and iodine concentration ratio between the arterial phase and portal venous phase had high sensitivity (77%) and specificity (87%) in differentiating healthy liver from cirrhosis (n = 81). A recent study by Sofue et al (23) evaluating 47 individuals showed good correlation (Spearman ρ = 0.65, $P < .001$) between NIC

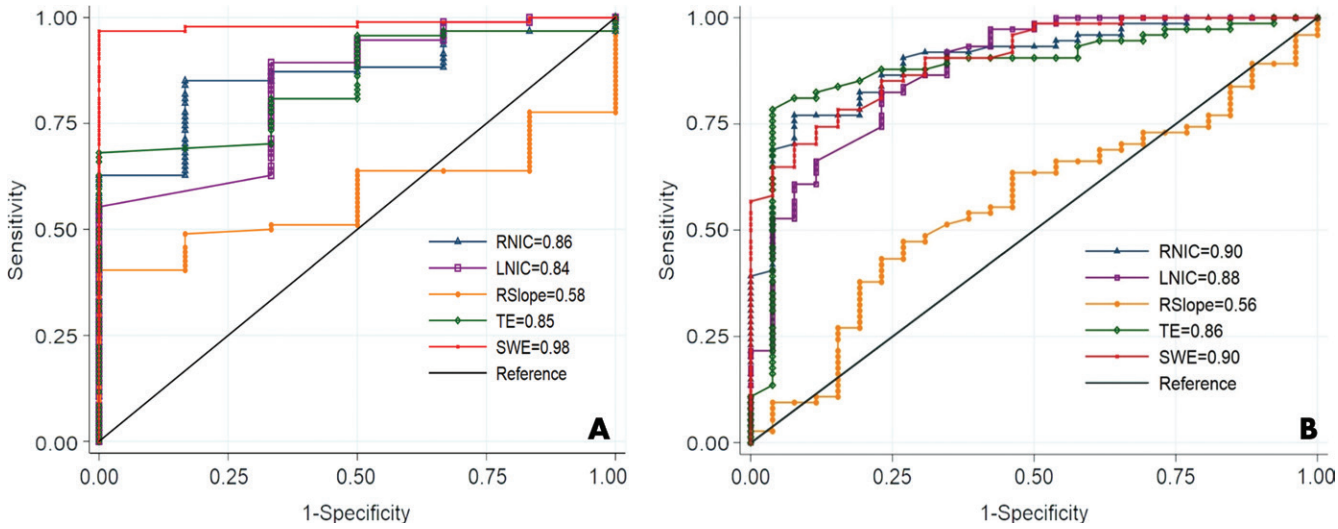

Figure 4: Graphs show comparison of area under the receiver operating characteristic curve (AUC) of normalized iodine concentration (NIC) of the right lobe of the liver (RNIC), NIC of the left lobe of the liver (LNIC), slope of monochromatic spectral curve (RSlope), and liver stiffness as measured with transient elastography (TE) and shear-wave elastography (SWE) in the differentiation of different groups of fibrosis. *A*, Graph compares stage F0 versus stage F1–F4 fibrosis. *B*, Graph compares stage F0–F1 versus stage F2–F4 fibrosis. Values mentioned are the AUC.

Table 3: Comparison of Cut-off Values of RNIC and Liver Stiffness as Measured with TE and SWE for Various Groups with Hepatic Fibrosis along with Sensitivity, Specificity, and Accuracy

Fibrosis Group and Quantitative Imaging Parameter	Cut-off Value	Sensitivity (%)	Specificity (%)	Accuracy (%)	AUC
≥F1					
RNIC	0.24	85 [77, 91] (86/101)	83 [42, 98] (84/101)	85 [59, 92]	0.86 [0.76, 0.97]
LS at TE	7.6 kPa	81 [72, 88] (82/101)	67 [30, 90] (68/101)	80 [49, 86]	0.85 [0.73, 0.97]
LS at SWE	6.3 kPa	97 [91, 99] (98/101)	100 [55, 100] (101/101)	97 [81, 99]	0.98 [0.96, 1.00]
≥F2					
RNIC	0.29	84 [74, 90] (67/80)	81 [63, 92] (65/80)	83 [73, 91]	0.90 [0.85, 0.97]
LS at TE	9.2 kPa	84 [74, 91] (67/80)	85 [66, 94] (68/80)	84 [69, 93]	0.89 [0.80, 0.97]
LS at SWE	8.6 kPa	80 [70, 87] (64/80)	82 [63, 92] (66/80)	80 [69, 91]	0.90 [0.84, 0.96]
≥F3					
RNIC	0.34	87 [74, 94] (40/46)	87 [76, 93] (40/46)	87 [77, 93]	0.93 [0.89, 0.99]
LS at TE	11.8 kPa	87 [71, 93] (40/46)	70 [57, 80] (32/46)	76 [66, 84]	0.83 [0.76, 0.92]
LS at SWE	11.1 kPa	83 [69, 91] (38/46)	78 [67, 87] (36/46)	80 [70, 88]	0.88 [0.82, 0.94]
≥F4					
RNIC	0.40	93 [68, 100] (14/15)	87 [76, 91] (13/15)	86 [71, 98]	0.96 [0.92, 1.00]
LS at TE	15 kPa	93 [64.2, 100] (14/15)	80 [68.6, 85.8] (12/15)	80 [67, 91]	0.90 [0.84, 0.97]
LS at SWE	13.5 kPa	73 [47.5, 89.3] (11/15)	80 [71, 87.3] (12/15)	79 [58, 87]	0.79 [0.69, 0.94]

Note.—Data in brackets are 95% CIs, and data in parentheses are numbers of participants. AUC = area under the receiver operating characteristic curve, LS = liver stiffness, RNIC = normalized iodine concentration of the right lobe of the liver, SWE = shear-wave elastography, TE = transient elastography.

in the 3-minute delayed DECT scans and METAVIR stages (Table 5). Whereas most studies have previously evaluated NIC at 3-minute delayed acquisition (18,23–25), we used 5-minute delayed acquisition. This was based on the rationale that fibrotic areas show gradual contrast material accumulation and that CT acquisition with a delay of more than 3 minutes would result in higher iodine concentrations in fibrotic livers. With sensitivity of 84%–93% and specificity of 81%–87% for RNIC, our results were better in staging fibrosis, and the RNIC cut-off values for different fibrosis stages had less overlap compared with prior work. Our study also compared RNIC with LS as measured with TE and SWE, which are other routinely used modalities, and its performance was not significantly different.

Although the slope of monochromatic spectral curve enabled the differentiation of cirrhosis (stage F4) from early stages of fibrosis (AUC = 0.79; 95% CI: 0.58, 0.87), it did not correlate with histologic assessment. Few studies have evaluated spectral curve slope in focal liver lesions such as hepatocellular carcinoma, hemangioma, abscess, and metastases

Table 4: Comparison of RNIC, TE, and SWE in the Differentiation of Early Stages of Fibrosis

METAVIR Stage	RNIC*	LS at TE (kPa)†	LS at SWE (kPa)‡
F0 (n = 6)	0.23 (0.18–0.24)	6.0 (4.5–9)	5.4 (4.5–5.5)
F1 (n = 21)	0.24 (0.21–0.28)	6.8 (5.5–8.7)	7.3 (6.5–8.3)
F1 (n = 21)	0.24 (0.21–0.28)	6.8 (5.5–8.7)	7.3 (6.5–8.3)
F2 (n = 34)	0.30 (0.27–0.33)	11.8 (8.9–14.3)	9.3 (7.5–12.8)

Note.—Numbers are medians, with the interquartile range in parentheses. LS = liver stiffness, RNIC = normalized iodine concentration of the right lobe of the liver, SWE = shear-wave elastography, TE = transient elastography.

* P = .60 for comparison of F0 versus F1, and P < .001 for comparison of F1 versus F2.

† P = .58 for comparison of F0 versus F1, and P < .001 for comparison of F1 versus F2.

‡ P = .002 for comparison of F0 versus F1, and P = .002 for comparison of F1 versus F2.

Table 5: Comparison of Cut-off Values of RNIC for Differentiation of Different Categories of Hepatic Fibrosis in Present Study versus a Previous Study

	F0 vs F1–F4		F0–F1 vs F2–F4		F0–F2 vs F3–F4		F0–F3 vs F4	
Parameter	Sofue et al	Present Study	Sofue et al	Present Study	Sofue et al	Present Study	Sofue et al	Present Study
Cut-off value	0.27	0.24	0.27	0.29	0.29	0.34	0.30	0.40
Sensitivity (%)	71.4	85	79.4	84	76	87	90	93
Specificity (%)	100	83	77	81	81.8	87	73	85
Accuracy (%)	74.5	85	78.7	83	78.7	87	76.6	86
AUC	0.81	0.86	0.80	0.90	0.82	0.93	0.86	0.96

Note.—The overall correlation coefficient of RNIC with fibrosis was 0.65 (P < .001) in Sofue et al (22) and 0.81 (P < .001) in the present study. AUC = area under the receiver operating characteristic curve, RNIC = normalized iodine concentration of the right lobe of the liver.

(26–28). To our knowledge, no prior study has studied it in liver fibrosis.

In addition to evaluating the accuracy of NIC for staging fibrosis, we compared its performance with that of LS at TE and SWE, which are used routinely in the evaluation of hepatic fibrosis owing to their high diagnostic performance in differentiating various fibrosis stages (AUC of 0.70–0.96 for TE and 0.77–0.98 for SWE) (29–31). We found that NIC derived from DECT was similarly accurate in discriminating fibrosis stages compared with SWE and TE, with no significant differences in AUCs.

DECT provides information related to the spatial distribution of fibrosis in the entire liver, in contrast to TE, SWE, or biopsy, which could assist in more accurate prognostication and enable identification of appropriate sites for biopsy (18). Studies have shown differential changes in volume and function between right and left lobes with the progression of liver disease (32,33). In our study, the mean LNIC values in individual fibrosis stages were slightly higher than RNIC values, particularly in the intermediate stages. However, the difference was not statistically significant.

Our study had limitations. The sample size and the number of participants in each METAVIR stage group were relatively small. The use of liver biopsy as a reference standard may itself be flawed because it can be affected by variability in sampling. The region in the liver where the NIC was measured may not have been the same as the area from which the biopsy specimen was obtained. Although attempts were made to match the area, some mismatch error was always possible. Interreader reproducibility of iodine concentration measurements at DECT was not evaluated, as analysis was done by two radiologists in consensus at the same time. However, the intraclass correlation coefficient showed good reliability of the values of RNIC and LNIC. There was a time gap (although <3 months) between DECT, TE, and biopsy, which could potentially have affected our results. Our investigational approach did not account for confounding factors such as patient's size, cardiac output, fatty liver, liver inflammation grade, hepatic iron accumulation, hematocrit level of the participant, and minor hepatic vascular pathologic conditions that could affect the iodine concentration in the liver and its measurement at DECT. No histologic information was available for control subjects, which may have explained the wider range of RNIC values in that group.

In conclusion, in chronic liver disease, the normalized iodine concentration in the liver at 5-minute delayed dual-energy CT (DECT) showed strong correlation with the histologic stages of fibrosis and good diagnostic performance in estimating liver fibrosis. Hence, implementation of a 5-minute delayed DECT scan instead of the standard 3-minute scan in the routine multiphase CT protocol for the evaluation of chronic liver disease would assist in seamless noninvasive staging of liver fibrosis.

Author contributions: Guarantors of integrity of entire study, U.K.M., K.S.M.; study concepts/study design or data acquisition or data analysis/interpretation, all authors; manuscript drafting or manuscript revision for important intellectual content, all authors; approval of final version of submitted manuscript, all authors; agrees to ensure any questions related to the work are appropriately resolved, all

authors; literature research, U.K.M., Shalimar, K.S.M.; clinical studies, P.D., Shalimar; experimental studies, P.D.; statistical analysis, U.K.M., M.K.; and manuscript editing, U.K.M., Shalimar, D.N.S., K.S.M.

Disclosures of Conflicts of Interest: **U.K.M.** disclosed no relevant relationships. **P.D.** disclosed no relevant relationships. **Shalimar** disclosed no relevant relationships. **M.K.** disclosed no relevant relationships. **D.N.S.** disclosed no relevant relationships. **K.S.M.** disclosed no relevant relationships.

References

1. Sebastiani G. Non-invasive assessment of liver fibrosis in chronic liver diseases: implementation in clinical practice and decisional algorithms. World J Gastroenterol 2009;15(18):2190–2203.
2. Moorman AC, Gordon SC, Rupp LB, et al. Baseline characteristics and mortality among people in care for chronic viral hepatitis: the chronic hepatitis cohort study. Clin Infect Dis 2013;56(1):40–50.
3. Liang R, Liu A, Perumpail RB, Wong RJ, Ahmed A. Advances in alcoholic liver disease: an update on alcoholic hepatitis. World J Gastroenterol 2015;21(42):11893–11903.
4. Bonis PA, Friedman SL, Kaplan MM. Is liver fibrosis reversible? N Engl J Med 2001;344(6):452–454.
5. Friedman SL. Liver fibrosis: from bench to bedside. J Hepatol 2003;38(Suppl 1):S38–S53.
6. Bravo AA, Sheth SG, Chopra S. Liver biopsy. N Engl J Med 2001;344(7):495–500.
7. Baranova A, Lal P, Birerdinc A, Younossi ZM. Non-invasive markers for hepatic fibrosis. BMC Gastroenterol 2011;11(1):91.
8. Chin JL, Pavlides M, Moolla A, Ryan JD. Non-invasive Markers of Liver Fibrosis: Adjuncts or Alternatives to Liver Biopsy? Front Pharmacol 2016;7:159.
9. Sun W, Cui H, Li N, et al. Comparison of FIB-4 index, NAFLD fibrosis score and BARD score for prediction of advanced fibrosis in adult patients with non-alcoholic fatty liver disease: a meta-analysis study. Hepatol Res 2016;46(9):862–870.
10. Salkic NN, Jovanovic P, Hauser G, Brcic M. FibroTest/Fibrosure for significant liver fibrosis and cirrhosis in chronic hepatitis B: a meta-analysis. Am J Gastroenterol 2014;109(6):796–809.
11. Ferraioli G, Tinelli C, Dal Bello B, et al. Accuracy of real-time shear wave elastography for assessing liver fibrosis in chronic hepatitis C: a pilot study. Hepatology 2012;56(6):2125–2133.
12. Barr RG, Ferraioli G, Palmeri ML, et al. Elastography Assessment of Liver Fibrosis: Society of Radiologists in Ultrasound Consensus Conference Statement. Radiology 2015;276(3):845–861.
13. Hoffman DH, Ayoola A, Nickel D, Han F, Chandarana H, Shanbhogue KP. T1 mapping, T2 mapping and MR elastography of the liver for detection and staging of liver fibrosis. Abdom Radiol (NY) 2020;45(3):692–700.
14. Besa C, Wagner M, Lo G, et al. Detection of liver fibrosis using qualitative and quantitative MR elastography compared to liver surface nodularity measurement, gadoxetic acid uptake, and serum markers. J Magn Reson Imaging 2018;47(6):1552–1561.
15. Yoshimitsu K, Mitsufuji T, Shinagawa Y, et al. MR elastography of the liver at 3.0 T in diagnosing liver fibrosis grades; preliminary clinical experience. Eur Radiol 2016;26(3):656–663.
16. Coursey CA, Nelson RC, Boll DT, et al. Dual-energy multidetector CT: how does it work, what can it tell us, and when can we use it in abdominopelvic imaging? RadioGraphics 2010;30(4):1037–1055.
17. Mendonca PRS, Lamb P, Sahani DV. A Flexible Method for Multi-Material Decomposition of Dual-Energy CT Images. IEEE Trans Med Imaging 2014;33(1):99–116.
18. Lamb P, Sahani DV, Fuentes-Orrego JM, Patino M, Ghosh A, Mendonça PRS. Stratification of patients with liver fibrosis using dual-energy CT. IEEE Trans Med Imaging 2015;34(3):807–815.
19. Lv P, Lin X, Gao J, Chen K. Spectral CT: preliminary studies in the liver cirrhosis. Korean J Radiol 2012;13(4):434–442.
20. Wei J, Zhao J, Zhang X, et al. Analysis of dual energy spectral CT and pathological grading of clear cell renal cell carcinoma (ccRCC). PLoS One 2018;13(5):e0195699.
21. Semelka RC, Chung JJ, Hussain SM, Marcos HB, Woosley JT. Chronic hepatitis: correlation of early patchy and late linear enhancement patterns on gadolinium-enhanced MR images with histopathology initial experience. J Magn Reson Imaging 2001;13(3):385–391.
22. Fuentes J, Patino M, Hayano K, Andrabi Y, Agrawal M, Sahani D. Detection and Stratification of Liver Fibrosis Using Dual Energy CT (DECT). Radiological Society of North America 2014 Scientific Assembly and Annual Meeting, Chicago IL. http://archive.rsna.org/2014/14015323.html. Accessed May 14, 2020.
23. Sofue K, Tsurusaki M, Mileto A, et al. Dual-energy computed tomography for non-invasive staging of liver fibrosis: accuracy of iodine density measurements from contrast-enhanced data. Hepatol Res 2018;48(12):1008–1019.
24. Yoon JH, Lee JM, Klotz E, et al. Estimation of hepatic extracellular volume fraction using multiphasic liver computed tomography for hepatic fibrosis grading. Invest Radiol 2015;50(4):290–296.
25. Guo SL, Su LN, Zhai YN, et al. The clinical value of hepatic extracellular volume fraction using routine multiphasic contrast-enhanced liver CT for staging liver fibrosis. Clin Radiol 2017;72(3):242–246.
26. Wang Q, Shi G, Qi X, Fan X, Wang L. Quantitative analysis of the dual-energy CT virtual spectral curve for focal liver lesions characterization. Eur J Radiol 2014;83(10):1759–1764.
27. Wang N, Ju Y, Wu J, et al. Differentiation of liver abscess from liver metastasis using dual-energy spectral CT quantitative parameters. Eur J Radiol 2019;113:204–208.
28. Qi X. Differentiating liver lesion types by DECT keV spectrum. ECR 2014 PosterNG. European Congress of Radiology 2014.. Accessed May 14, 2020.
29. Foucher J, Chanteloup E, Vergniol J, et al. Diagnosis of cirrhosis by transient elastography (FibroScan): a prospective study. Gut 2006;55(3):403–408.
30. Cardoso AC, Carvalho-Filho RJ, Stern C, et al. Direct comparison of diagnostic performance of transient elastography in patients with chronic hepatitis B and chronic hepatitis C. Liver Int 2012;32(4):612–621.
31. Gaia S, Carenzi S, Barilli AL, et al. Reliability of transient elastography for the detection of fibrosis in non-alcoholic fatty liver disease and chronic viral hepatitis. J Hepatol 2011;54(1):64–71.
32. Ozaki K, Matsui O, Kobayashi S, Minami T, Kitao A, Gabata T. Morphometric changes in liver cirrhosis: aetiological differences correlated with progression. Br J Radiol 2016;89(1059):20150896.
33. Matsuzaki S, Onda M, Tajiri T, Kim DY. Hepatic lobar differences in progression of chronic liver disease: correlation of asialoglycoprotein scintigraphy and hepatic functional reserve. Hepatology 1997;25(4):828–832.